



A NOVEL THREE- PORT DC-DC CONVERTER PV/BATTERY CONNECTED POWER SYSTEMS

KALATTURU SESHU

Pg scholar, Chadalawada Ramanamma Engineering College, Tirupati, kalatturu.seshu@gmail.com

M. LAKSHMI KANTH REDDY

Associate.Professor, Chadalawada Ramanamma Engineering College, Tirupati, Lkreddy.eee@gmail.com

ABSTRACT- A three port DC-DC Converter integrating photovoltaic (PV) and battery power for high step-up applications is proposed in this paper. The topology includes five MOSFETs, two coupled inductors, and two active clamp circuits. Maximum power point tracking (MPPT) algorithm is used to extract the maximum available power from PV module under certain conditions. As long as the sun irradiation is high, MPPT is enabled and if the power generated by the PV panel is much greater than the load demand, it is used to charge the batteries. MPPT algorithm is disabled only when the battery charging voltage is too high, so as to prevent it from overcharging. Different load conditions, load change conditions and mode change conditions are simulated and studied in this paper. The three-port converter integrating the PV and battery is synchronised and connected to a local grid.

Keywords-DC microgrid, PV panel, battery storage MPPT algorithm, High step-up application, grid connected system, three port converter.

1.INTRODUCTION

As the world population is increasing rapidly, the power demand and the load demand is also increasing rapidly. Renewable energy sources hold a vital role in generating the power and meeting with the load demands. With surplus advantages like low or almost nil harmful emissions, reliability, durability and low maintenance, renewable energy sources are now playing a major role in satisfying the future energy demand. However, owing to few disadvantages like fluctuation in output due to climatic conditions, irradiance, and temperature and so on, renewable energy sources are still under the research area. To cope up with the drawbacks batteries are used as storage mechanism for smoothing output power, improving start up transitions and dynamic characteristics, and enhancing the peak power capacity. For this purpose hybrid power system combining PV, battery, etc are being proposed. These hybrid power systems have the potential to provide high quality, more

reliable and efficient power. Many hybrid power systems with various power electronic converters have been proposed in the literature up to now. However, the main shortcomings of these integrating methods are complex system topology, high count of devices, high power losses, expensive cost, and large size [1].

Integrated multi port converters are used to interface power sources with storage devices. They have the advantages like less components, lower cost, more compact size, and better dynamic performance. In many cases, at least one energy storage device should be incorporated. For example, in the electric vehicle application, the regenerative energy occurs during acceleration or start up. Therefore, it is very important for the port connected to the energy storage to allow bidirectional power flow. Various kinds of topologies have been proposed due to the advantages of multiport converters. The combination strategies for the multiport converter include sharing switches, capacitors, inductors, or magnetic cores [2]. One could select a proper topology by considering many aspects such as cost, reliability, and flexibility depending on the applications. An application of hybrid energy supply using renewable energy sources and storage devices is discussed in [3]. The dc microgrid enabled by the solid-state transformer (SST) in the Future Renewable Electric Energy Delivery and Management System (FREEDM System) integrates various distributed renewable energy resources (DRERs) and distributed energy storage devices (DESDs) [4]. For instance, if solar power is selected as the renewable energy source and battery as the storage device, the battery can either supply the load with the solar energy at the same time or store the excess power from the solar panels for backup use. Therefore, the bidirectional power path must be provided for the battery port. The dc-dc converters interfacing the DRERs or DESDs are expected to have relative high voltage conversion ratios since the dc bus of the FREEDM system is 380 V. It is studied that for the dc-dc converters connected to the solar panels, voltage gain extension cells such as coupled

inductors, transformers, and switched capacitors are often employed to achieve high voltage conversion ratios [5]. By utilizing the voltage gain extension cells, the extreme duty cycles that exist in typical boost converters can be avoided and the voltage stress on switches can be reduced. Thus, power switches with lower voltage rating and lower turn-on resistance can be chosen for the converters to reduce conduction losses.

The topology of the proposed model of three port dc-dc converter for grid connected PV/battery power systems is shown in the Fig.1. A grid connected system is that which works in with the local utility grid so that when the solar produces more electricity than a house is using the surplus power is fed into the grid. If the house requires more power than what the solar panels are producing then the balance of the electricity is supplied by the utility grid. With a standalone solar system the solar panels are not connected to a grid but instead are used to charge a bank of batteries. This set up is used in areas where no public grid is available. But the growth in solar power systems in the last five years has been in the grid connected systems. Because most people live in areas that are connected to a public grid and stand-alone systems are much, much more expensive than the grid connected systems because the batteries are very dear. A grid connected system needs to synchronise input to the grid.

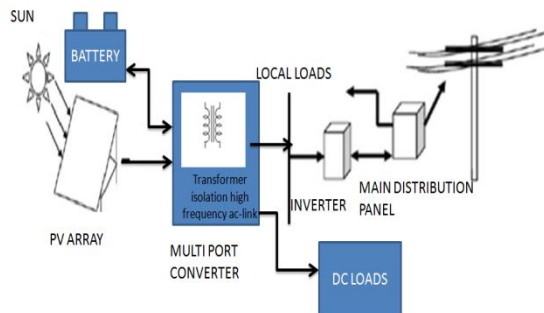


Fig.1. Block Diagram Of a Three Port Dc-DC Converter for Grid-connected PV/Battery Power Systems

Many multiport converter topologies have been presented in the literature and can be roughly divided into two categories. One is non isolated type [6]–[9]: the non isolated converters are usually derived from the typical buck, boost, or buck–boost topologies and are more compact in size. The other is isolated type [28]–[30]: the isolated converters using bridge topologies and multi winding transformers to match wide input voltage ranges.

In this paper, a high step-up three-port dc-dc converter for the hybrid PV/battery system is proposed with the following advantages:

- 1) High voltage conversion ratio is achieved by using coupled inductors;

- 2) Simple converter topology which has reduced number of the switches and associate circuits;
- 3) Simple control strategy which does not need to change the operation mode after a charging/discharging transition occurs unless the charging voltage is too high; and
- 4) Output voltage is always regulated at 380V under all operation modes.

The major contribution of this paper is to propose an integrated three-port converter as a non isolated alternative other than typical isolated topologies for high step-up three-port applications. The proposed switching strategy allows the converter to be controlled by the same two duty cycles in different operation modes. The detailed analysis is given in the following sections: The principle of operation is described in Section II. The PV source modelling and battery modelling is given in Section III. The control strategy is explained in Section IV. Finally, the simulation results are presented in Section V.

II. PRINCIPLE OF OPERATION

This section introduces the topology of proposed non isolated three-port dc-dc converter, as illustrated in Fig. 2. The converter is composed of two main switches S_1 and S_2 for the battery and PV port. Synchronous switch S_3 is driven complementarily to S_1 such that bidirectional power flow for the battery port can be achieved. Two coupled inductors with winding ratios n_1 and n_2 are used as voltage gain extension cells. Two sets of active-clamp circuits formed by S_4, L_{k1}, C_{c1} and S_5, L_{k2}, C_{c2} are used to recycle the leakage energy. L_{k1} and L_{k2} are both composed of a small leakage inductor from the coupled inductor and an external leakage inductor. Two independent control variables, duty cycles d_1 and d_2 , allow the control over two ports of the converter, while the third port is for the power balance. The fixed-frequency driving signals of the auxiliary switches S_3 and S_4 are complementary to primary switch S_1 . Again, S_3 provides a bidirectional path for the battery port. Similarly, S_5 is driven in a complementary manner to S_2 . A 180° phase shift is applied between the driving signals of S_1 and S_2 .

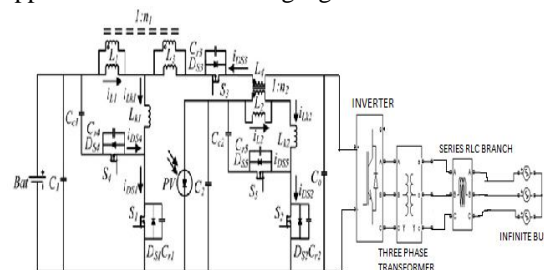


Fig 2. Topology of the proposed converter

There are four operation periods based on the available solar power. First, the sun is in the eclipse stage and the solar irradiation is either unavailable or very low.

This operation period is defined as period 1, and the battery will serve as the main power source. As the sun starts to shine and the initial solar irradiation is enough for supplying part of the load demand, the operation period is changed to period 2. The load is supplied by both solar and battery power in this period. For period 3, the increasing isolation makes the solar power larger than the load demand. The battery will preserve extra solar power for backup use. During period 4, the charging voltage of the battery reaches the preset level and should be limited to prevent overcharging. According to the solar irradiation and the load demand, the proposed three-port converter can be operated under two modes. In the battery balance mode (mode 1), maximum power point tracking (MPPT) is always operated for the PV port to draw maximum power from the solar panels. The battery port will maintain the power balance by storing the unconsumed solar power during light-load condition or providing the power deficit during heavy-load condition. The power sharing of the inputs can be represented as

$$P_{load} = P_{PV_SVC} + P_{bat_SVC} \quad (1)$$

Where P_{load} is the load demand power, P_{PV_SVC} is the PV power under solar voltage control (SVC), and P_{bat_SVC} is the battery power under SVC. In mode1, maximum power is drawn from the PV source. The battery may provide or absorb power depending on the load demand. Therefore, P_{bat_SVC} could be either positive or negative. When the battery charging voltage is higher than the maximum setting, the converter will be switched into battery management mode (mode2). In, mode2, MPPT will be disabled; therefore, only part of the solar power is drawn. However, the battery voltage could be controlled to protect the battery from overcharging. The power sharing of the inputs can be represented as

$$P_{load} = P_{PV_BVC} + P_{bat_BVC} \quad (2)$$

Where P_{PV_BVC} is the PV power under battery voltage control (BVC) and P_{bat_BVC} is the battery charging power under SVC. If the load is increased and the battery voltage is reduced, the converter will be switched to mode 1. The output voltage is always kept at 380 V in both modes.

III. PV SOURCE AND BATTERY MODELLING

The PV source modelling is clearly explained in [3] and the battery used here is the Nickel-metal-hydride battery. The purpose of using this battery is given in [13]. NiMH batteries provide the following advantages over NiCd:

- Higher capacity
- Limited memory effect

- Environmentally friendly

The comparison of different batteries is given in Table I.

IV. CONTROL STRATEGY

As mentioned in Section II, the operation modes of the converter are determined by the conditions of available solar power and battery charging states. Controlling the converter in each mode requires different state variables to regulate voltages of the input and output ports. There are three control loops for the proposed converter: output voltage control (OVC), SVC, and BVC. The control scheme is shown in Fig.4. The OVC is a simple voltage regulation loop. The SVC and BVC loops share the same control variable d_2 to achieve smooth mode transitions. SVC is used to regulate the voltage of the PV port and implement the MPPT algorithm. BVC is the battery voltage regulation loop to prevent overcharging. It is noted that the PV port is operated under SVC most of the time. Therefore, BVC would not be active under normal operation. Only one control loop between SVC and BVC is performed. Moreover, once BVC starts to take control over d_2 , SVC will be disabled immediately to avoid the noise issue caused by the MPPT algorithm.

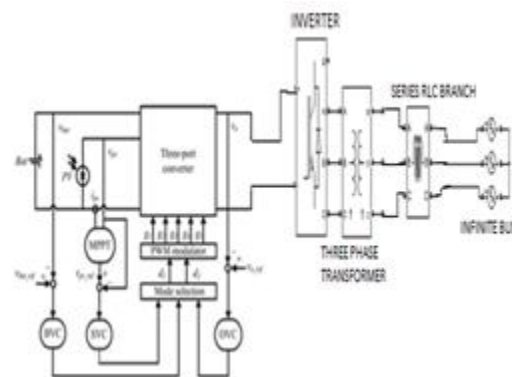


Fig 4. Control scheme of the proposed three port converter

Table I – Comparison of NiCd, NiMH, and Li-Ion Batteries.

PARAMETER	NiCd	NiMH	Li-ion
Relative Capacity	1	1.4	3
Charge/Discharge Cycle Life	500+cycles	500+cycles	300+cycles
Memory Effect	Noticeable effect. Can Be eliminated by periodic conditioning	Little effect	No memory effect
Conditioning	Recommended periodically to eliminate memory	Recommended when new and after long storage periods	Not necessary
Operating Temperature	-22 to+140°F (-30 to +60°C)	-4 to +122 °F (-20 to +50°C)	+14 to +122°F (-10 to+50°C)
Charging Temperature	+32 to 113°F (0 to +45°C)	+32 to +113°F (0 to +45°C)	+32 to +104°F (0 to+40°C)
Storage Temperature(>90 days)	+32 to +86°F (0 to +30°C)	+32 to +86°F (0 to +30°C)	+32 to +86°F (0 to +30°C)
High-Temperature Susceptibility	Some permanent loss of capacity above 140°F (60°C)	Greater permanent loss of capacity above 140°F (60°C)	Greater permanent loss of capacity above 140°F (>60°C)
Self-Discharge	20% loss of charge/month at 77°F (25°C)	30% loss of charge/month at 77°F (25°C)	Self-discharge much lower than Nickel chemistries.
Recycling	Required by law in the U.S.	Not Required, but recommended	Not Required.

PARAMETER	VALUE
V_{bat}	48V
V_{pv_OC} (@800W/m ²)	52.8V
V_O	380V
P_{PV_max} (@800W/m ²)	200W
P_{o_max}	200W
f_{sw}	50kHz
n_1, n_2	4.44
L_1, L_2	52μH
L_{K1}, L_{K2}	1μH
C_{C1}, C_{C2}	470μF
C_o	47μF

Table II: CIRCUIT PARAMETERS

V.SIMULATION RESULTS

Simulation results are carried out to analyze and study the performance of the three port converter under various conditions. The parameters of the circuit are set according to that given in Table II. The output is studied when there are low load conditions, high load conditions, change in load condition, mode transitions i.e.; from mode1 (PV mode)to mode 2 (battery mode) and vice versa.

The simulink model for the proposed topology of the three port converter using PV and battery as the inputs is shown in fig 5(a). The converter integrating PV and battery as inputs is in then fed to a local grid. The control scheme

for the proposed topology is given in fig 5(b).

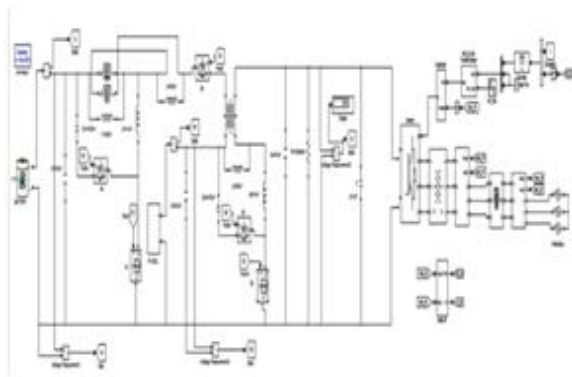


Fig 5(a) : Simulink model of the proposed topology connected to a grid.

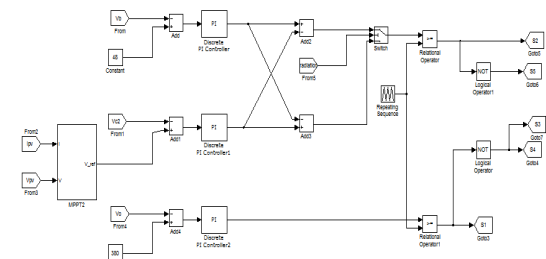


Fig 5(b) : Control circuitry of the proposed topology.

In Fig. 6, the sun radiation is in period 1. For the first 10 s, there is very little sunlight i.e., during the initial part of the day, so the MPPT is performed. However, once the level is too low or not available, MPPT is then disabled and the battery will become the only power source to supply the load. After 10 sec, PV power increases and there's a sudden increase in I_{pv} and now the battery starts to store the surplus power coming from the PV, and hence gets charged.



Fig. 6. Measured waveforms of mode operation in period 1 $R = 1204 \Omega$, (Ch1: V_o , Ch2: V_b , Ch3: I_b , Ch4: I_{pv})

The Simulink model and the control circuit for high

load condition is same as that of 5(a) and 5(b), except that the load is set to be of 3030 ohms.

In Fig. 7, for the first 20sec the sun irradiation is not too high. The solar port is operated under MPPT and the battery port is discharged to supply part of the load. As the irradiation increases, the PV port will generate more power than the battery port.

The increasing sun irradiation reaches a high after 20 sec. The power generated from the PV port is now larger than the load demand, so the battery port should be charged to store additional power. Although the batteries are charged, the charging voltage is not high enough to trigger the BVC loop. Thus, the solar panels still work under MPPT. As shown in Fig 7, the maximum charging voltage for the batteries is reached. The BVC loop is then active to regulate the charging voltage and the MPPT is disabled.

For load change conditions, the Simulink model is the same as in 5(a) except that the load is replaced by a converter subsystem as shown in fig 8 (a).

At the beginning of Fig.9, the load demand is set as 120W ($R = 1204\Omega$), the solar port is generating its maximum power and the deficit is provided by the battery port. At the time $t \approx 6$ s, load demand is decreased to 72 W ($R = 2000\Omega$), which is lower than the power generated from the solar panels.

The maximum solar power is still drawn from the panel after the load change and the batteries are charged by the additional solar power. It is observed that the current ripple of the battery is larger at the boundary of charging and discharging operations.

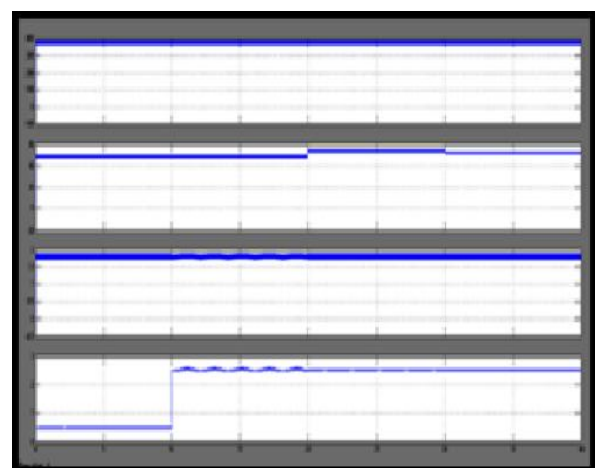


Fig 7. Measured waveforms of mode operation in period 1 ($R = 3030 \Omega$, Ch1: V_o , Ch2: V_b , Ch3: I_b , Ch4: I_{pv})

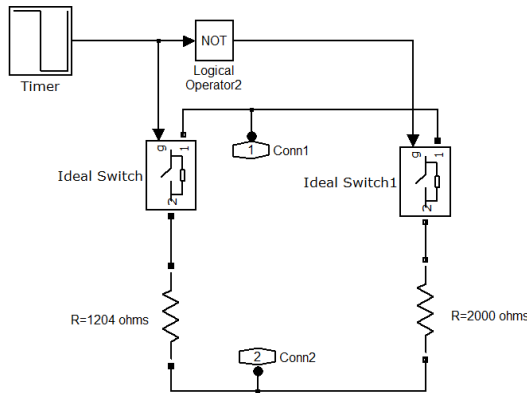


Fig 8(a): Converter subsystem for load change conditions.

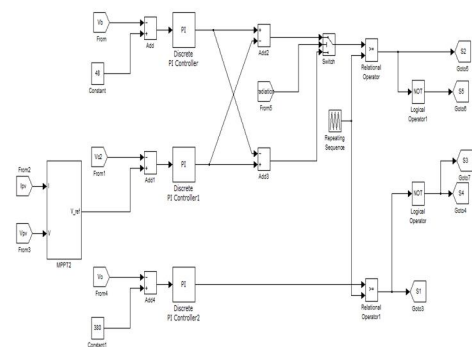


Fig 8(b): Control circuitry of the load change condition
When $t \approx 12$ s, the load is switched back to 120W, so the batteries are discharged again. It can be observed that the solar port works under MPPT as long as the battery voltage is not too high. The transitions of the battery between charging and discharging are smooth and the operation mode does not need to be changed. It should be noted that even during the load change, MPPT is achieved and the output voltage is well regulated. This is one of the important features of three-port converters since MPPT and load regulation could not be maintained simultaneously for typical two-port converters.

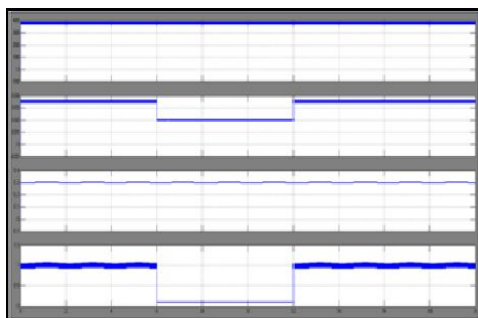


Fig 9 :Measured waveforms of load change condition (Ch1: Vo, Ch2: Vb, Ch3: Ib, Ch4: Ipv).

Figure 10 (a) and 10(b) show the Simulink model and control circuitry respectively for mode transition from mode 1(PV) to mode 2(battery) and vice versa.

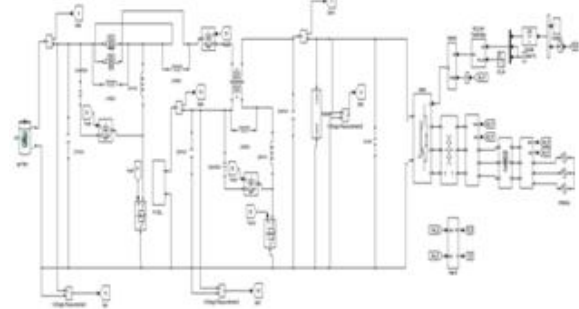


Fig 10(a): Simulink model for mode transition.

The subsystem 1 is the battery subsystem and the subsystem 2 is the PV subsystem. Fig.11 shows mode transition from SVC (mode1:MPPT, $R=900\Omega$) to BVC (mode 2: Battery voltage regulation, $R=3600\Omega$) when the maximum charging voltage is reached. The PV port is operated under MPPT at the beginning to generate Maximum solar power and the battery is discharged to share part of the load demand. It is noted that in mode 1, sometimes the solar power is slightly larger than the load demand; therefore, the batteries are temporally charged.

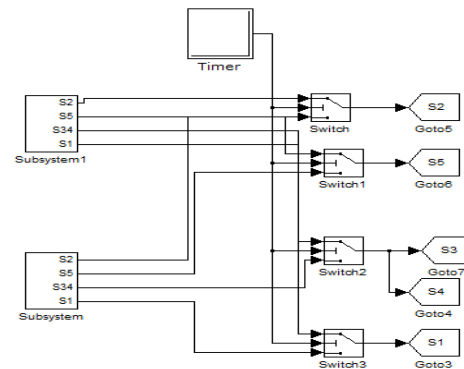


Fig 10(b): Control circuitry for mode transitions.

The battery voltage in this case is clearly higher than discharging situation. However, the charging voltage during this short period is not high enough, so the converter is still operated in mode 1. When a load change (from 80% to 20%) happened at $t \approx 5$ s; the battery is suddenly charged with a large current and the battery voltage is then increased dramatically. When the charging voltage is higher than the maximum setting, the operation mode is switched to mode 2 immediately to regulate the battery voltage and prevent overcharging. It can be seen that in mode 2, the solar panel is no longer operated around the maximum power point but the right side of it.

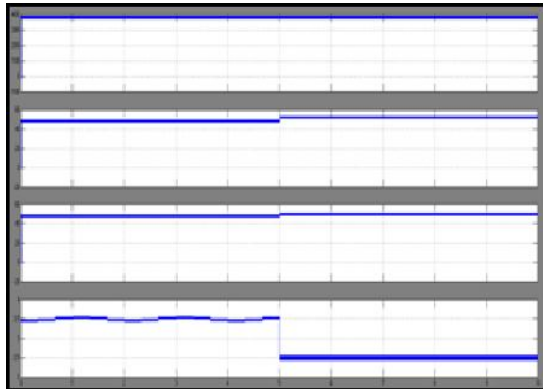


Fig. 11. Measured waveforms of mode transition (mode1–mode 2)(Ch1:Vo, Ch2:I_o, Ch3:Ipv, Ch4:I_b)

Fig. 12 shows the transition from mode 2 to mode 1 when the load is suddenly increased. The SVC will take over the control on the PV port since the maximum setting of the battery voltage could not be met. Similarly, sometimes the batteries could be slightly charged according to the intensity of solar irradiation. Again, no matter what mode is operated for the PV port, the output voltage will be always regulated at 380 V.

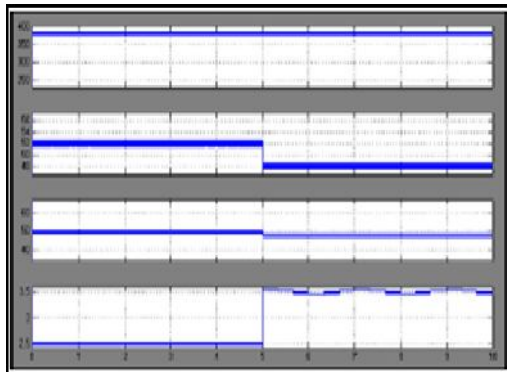


Fig. 12. Measured waveforms of mode transition (mode2–mode1) (Ch1:Vo, Ch2:I_o, Ch3:Ipv, Ch4:I_b)

VI. CONCLUSION

A high step-up three-port DC-DC converter for grid connected power systems is proposed to integrate solar and battery power. The model is developed and evaluated for different load conditions, mode change conditions etc.. The simulation results validate the functionality of the proposed converter under different solar irradiation level and load demand. The charging/discharging transitions of the battery could be achieved without changing the operation mode; therefore, the MPPT operation will not be interrupted. In light-

load condition, once the charging voltage is higher than the preset level, the operation mode will be changed rapidly to protect the battery from overcharging. To prevent the battery from overcharging different kinds of methods could be used as a future extension.

REFERENCES

- [1] X. Huang, X. Wang, T. Nergaard, J. S. Lai, X. Xu, and L. Zhu, "Parasitic ringing and design issues of digitally controlled high power interleaved boost converters," *IEEE Trans. Power Electron.*, vol. 19, No. 5, pp. 1341–1352, Sep. 2004.
- [2] S. H. Choung and A. Kwasinski, "Multiple-input DC-DC converter topologies comparison," in *Proc. 34th Annu. Conf. IEEE Ind. Electron.*, 2008, pp. 2359–2364.
- [3] Yen-Mo Chen, Student Member, IEEE, Alex Q. Huang, Fellow, IEEE, and Xunwei Yu, Student Member, IEEE] A High Step-Up Three-Port DC-DC Converter for Stand-Alone PV/Battery Power Systems *IEEE TRANSACTIONS ON POWER ELECTRONICS*, VOL. 28, NO. 11, NOVEMBER 2013
- [4] A. Huang, "FREEDM system—a vision for the future grid," in *Proc. IEEE Power Energy Soc. Gen. Meet.*, 2010, pp. 1–4.
- [5] W. Li and X. He, "Review of non isolated high-step-up DC/DC converters in photovoltaic grid-connected applications," *IEEE Trans. Ind. Electron.*, vol. 58, no. 4, pp. 1239–1250, Apr. 2011.
- [6] W. G. Imes and F. D. Rodriguez, "A two-input tri-state converter for space craft power conditioning," in *Proc. AIAA Int. Energy Convers. Eng. Conf.*, 1994, pp. 163–168.
- [7] F. D. Rodriguez and W. G. Imes, "Analysis and modeling of a two input DC/DC converter with two controlled variables and four switched networks," in *Proc. AIAA Int. Energy Conf.*, 1994, pp. 163–168.
- [8] B. G. Dobbs and P. L. Chapman, "A multiple-input DC-DC converter topology," *IEEE Power Electron. Lett.*, vol. 1, no. 1, pp. 6–9, Mar. 2003.



[9] R.J. Wai, Ch.Y. Lin, J. J. Liaw, and Y. R. Chang, "Newly designed ZVS multi input converter," IEEE Trans.Ind.Electron.,vol.58,no.2,pp.555–566,Feb2011.

[10] S. Yu and A. Kwasinski, "Analysis of a soft-switching technique for isolated time-sharing multiple-input converters," in Proc. IEEE Appl. Power Electron. Conf.,2012,pp.844–851.

[11] D. Liu and H. Li, "A ZVS bi-directional DC–DC converter for multiple energy storage elements," IEEE Trans. Power Electron., vol. 21, no. 5, pp.1513–1517,Sep. 2006.

[12] H. Tao, A. Kotso poulos, J. L. Duarte, and M. A. M. Hendrix, "Triple half-bridge bidirectional converter controlled by phase shift and PWM," in Proc. IEEEAppl. Power Electron. Conf., Mar. 2006,pp. 1256–1262.

[13] Comparison of NiCd, NiMH, and Li-Ion Batteries
[https://www.google.co.in/
Comparison+of+NiCd%2C+NiMH%2C+and+Li-Ion+Batteries.](https://www.google.co.in/Comparison+of+NiCd%2C+NiMH%2C+and+Li-Ion+Batteries)